$Cr(CO)_5$(phen) as an intermediate of photochemical CO substitution in $Cr(CO)_6$ with 1,10-phenanthroline[1]

Shigero Oishi

Department of Chemistry, School of Hygienic Sciences, Kitasato University, Kitasato, Sagamihara, Kanagawa 228 (Japan)

ABSTRACT

$Cr(CO)_5$(phen) generated as an intermediate of photochemical carbonyl substitution in $Cr(CO)_6$ with 1,10-phenanthroline (phen) has been investigated by laser flash photolysis with infrared detection. The $Cr(CO)_5$ moiety was found to have a square-pyramidal structure by analyzing with the Cotton-Kraihanzel force field. Simulation, based on the correlation of CO-stretching force constants with the bond indices calculated by ZINDO-MO, revealed that phen coordinated unusually in a monodentate fashion and the interaction between Cr and another nitrogen was antibonding.

INTRODUCTION

Ultraviolet irradiation of a solution of $Cr(CO)_6$ in the presence of bidentate ligand (bid) gives $Cr(CO)_4$(bid) as a final product. The reaction proceeds through the following steps.[2-6]

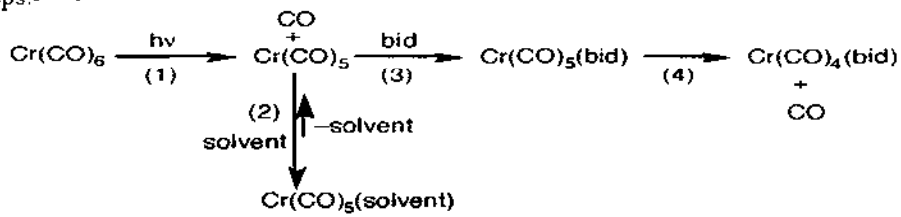

Even with a ligand as well-suited to bidentate bonding as phen, Step (3) did not concert with Step (4); $Cr(CO)_5$(phen) could be observed on visible absorption spectra in microsecond to millisecond time scales.[4] Though significant interactions between Cr and the "non-coordinating nitrogen" were suggested from the facts that the transient had an absorption maximum at a longer wavelength as compared with $Cr(CO)_5$(pyridine) and the acceleration of rate appeared both in Step (3) and (4), detailed information about the structure of the intermediate could not be obtained from the transient visible spectra.[4,6] We wish to report here the results obtained by time-resolved infrared spectroscopy.

0010-8545/94/$26.00
SSDI 0010-8545 (94) 02019-F

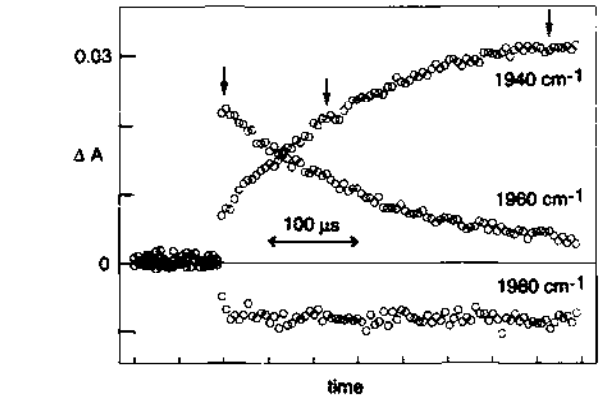

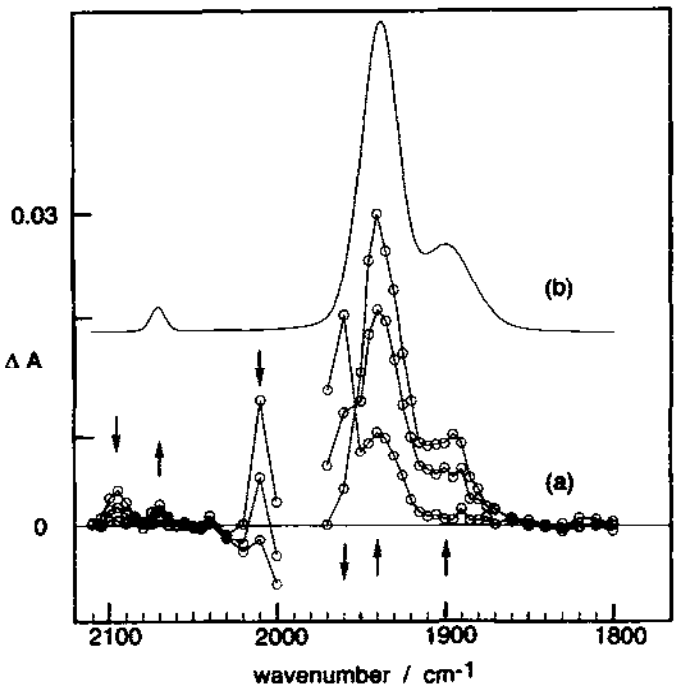

Fig. 1(top). Typical reaction traces by laser flash photolysis of trichloroethylene solutions of $Cr(CO)_6$ (4.0 mM) and phen (15.0 mM) under argon. A trace at 1980 cm^{-1} was obtained for a 2.0 mM solution of $Cr(CO)_6$. Points indicated by arrows were picked up for making time-resolved infrared spectra. Reproduced with permission from ref. 8.

Fig. 2(bottom). (a) Time-resolved infrared spectra just after the laser pulse, at 130 μs, and at 370 μs. Spectral changes with time are indicated by arrows. Bleaching at around 1980 cm^{-1} due to the photolysis of $Cr(CO)_6$ is not shown. (b) Simulation spectrum for $Cr(CO)_5$(phen) assuming a square-pyramidal structure of $Cr(CO)_5$ moiety. Reproduced with permission from ref. 8.

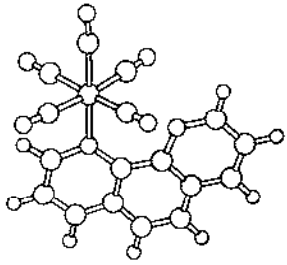

Capped octahedron

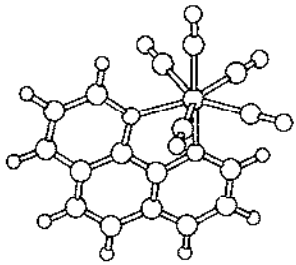

Pentagonal bipyramid

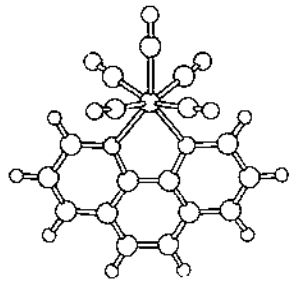

Octahedral wedge

RESULTS AND DISCUSSION

Trichloroethylene was used as a solvent for time-resolved infrared spectroscopy, since it is transparent in the region of CO-stretching and the UV-VIS spectral observations obtained in benzene[4] could be reproduced. Solutions of $Cr(CO)_6$ (4.0 mM) and phen (15.0 mM) were deaerated by bubbling argon for 20 min and then subjected to photolysis using the third harmonic of Nd-YAG laser (355 nm).[7,8] Typical reaction traces are shown in Fig. 1. At 1980 cm^{-1} where the starting $Cr(CO)_6$ has an absorption for CO-stretching, a swift bleaching takes place and continues throughout the time range, indicating the consumption of $Cr(CO)_6$. An absorption at 1960 cm^{-1} which appeared just after the laser pulse decayed with a pseudo-first order rate constant 4.98×10^3 s^{-1}, which is in good agreement with that for the increase of absorption at 1940 cm^{-1} (4.81×10^3 s^{-1}). Points corresponding to 0, 130, and 370 μs after the laser pulse, indicated by arrows in Fig. 1, were collected with varying wavenumber to compose differential infrared spectra (Fig. 2a). As an isosbestic point can be seen at 1955 cm^{-1}, the species just after the laser pulse clearly changes to the next one. These were consistent with the results in benzene observed at UV-VIS region.[4] Namely, the spectral change in Fig. 2a coincides with the conversion of $Cr(CO)_5$(trichloroethylene) to $Cr(CO)_5$(phen), which shows three peaks at 2070, 1940, and 1900 cm^{-1} with weak, strong, and medium intensities, respectively, characteristic of a square-pyramidal structure of $M(CO)_5$ fragment.

Under the approximation of Cotton-Kraihanzel force field (CKFF), force constants calculated from the application of the Timney's empirical equation to an assumed square-pyramidal structure of $Cr(CO)_5$ moiety were optimized to give a simulation spectrum shown in Fig. 2b, where axial-equatorial bond angles = 90.4°, a dipole derivative ratio $\mu_{ax}'/\mu_{eq}' = 1$, and the force constants (Nm^{-1}) $k_{ax} = 1478$, $k_{eq} = 1580$, $k_{ax,eq} = 38$, $k_{eq,eq} = 33$, $k_{trans} = 62$.[9-11] The observed bands at 2070, 1940, and 1900 cm^{-1} were assigned to the $A_1^{(1)}$ (2070 cm^{-1}), E (1939 cm^{-1}), and $A_1^{(2)}$ (1898 cm^{-1}) fundamentals, respectively. The frequency for the B_1 fundamental which is infrared inactive was calculated as 1975 cm^{-1}.

As for the whole structure of the transient including phen, we can expect three types of structure, namely, capped octahedron, pentagonal bipyramid, and octahedral wedge, as shown above, which were proposed as structures in transition states for the associative

substitution reaction in octahedral coordination compounds.[12,13] We tried to make simulation spectra for these structures by estimating force constants from the bond indices (Wiberg)[14] calculated with ZINDO/S-MO.[15]

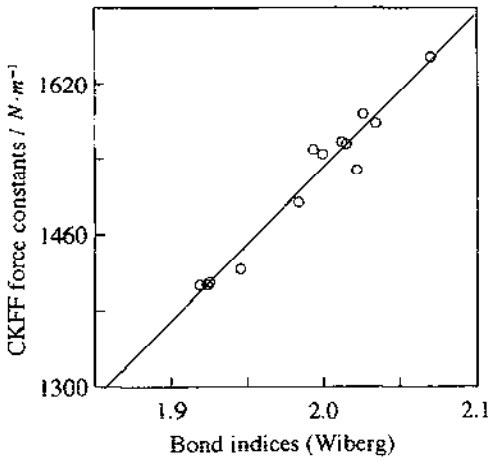

Fig. 3. Correlation of CKFF force constants with the bond indices for seven chromium carbonyls (thirteen types of carbonyl), $Cr(CO)_6$, $Cr(CO)_5$(pyridine), $Cr(CO)_4$(phen), $Cr(CO)_5I^-$, $Cr(CO)_5Br^-$, $Cr(CO)_5Cl^-$, and $Cr(CO)_5(PPh_3)$. The force constants for $Cr(CO)_5$(pyridine) and $Cr(CO)_4$(phen) were obtained in this work and the others were in ref. 9 and 16. The bond indices were calculated for structures optimized with using the standard MM2 parameters augmented in CAChe work system.[15]

As can be seen in Fig. 3, there is a good correlation between the CKFF force constants and the bond indices, indeed, the correlation coefficient = 0.977. Optimization for structures of capped octahedron, pentagonal bipyramid, and octahedral wedge was made in the same way as in Fig. 3 and then ZINDO/S calculation for these gave the bond indices, which in turn gave force constants for the diagonal components of F matrix. The interaction force constants were estimated by Timney's empirical equation and its interpolation.[10] Assuming a dipole derivative ratio = 1 and a half-width of band = 15 cm^{-1}, we obtained simulation spectra shown in Fig. 4. If we assume a pentagonal bipyramid for $Cr(CO)_5$(phen), phen cannot occupy two corners of pentagon because of congestion in the plane. The pentagonal bipyramid shown above, in which phen occupies one corner of pentagon and one of the tops of bipyramid, gave the simulation spectrum which consisted of five bands, being excluded as the structure for the intermediate. For the octahedral wedge structure, force constants for axial and equatorial carbonyls were determined as 1273 and 1490 Nm^{-1}, indicating weak CO bonds resulted from π donation of phen. Both the symmetric vibration which consisted mainly of an axial carbonyl stretching (1756 cm^{-1}) and the antisymmetric vibrations of equatorial carbonyls (1873 cm^{-1}) appeared at extremely low wavenumbers. These cannot satisfy the experimental spectrum. In the capped octahedron, the force constants for equatorial carbonyls close to a "cap" nitrogen (1538 Nm^{-1}) differed slightly with those for the others (1559 Nm^{-1}). Therefore, the B_1 fundamental, which should be infrared inactive, appeared at 1955 cm^{-1} as a weak band. Unfortunately, this fundamental may hide behind the bleaching in the experimental spectra. On the whole, the simulation spectrum for the capped octahedron is a good reproduction of the experimental one. The ZINDO/S calculation for this geometry rationalized the observed acceleration in Step (3) and (4) and the transient spectrum at visible region[4,6] as follows.

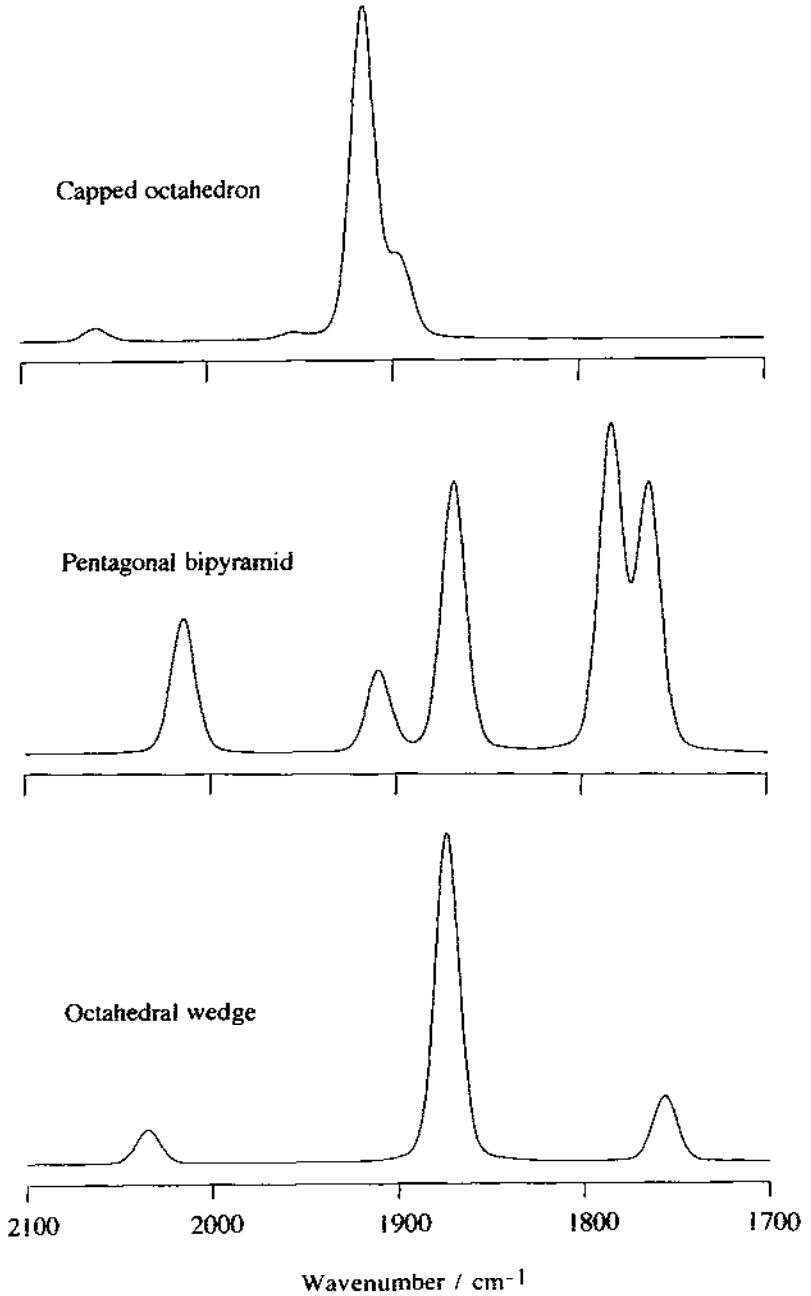

Fig. 4. Simulation spectra for capped octahedron, pentagonal bipyramid, and octahedral wedge geometry.

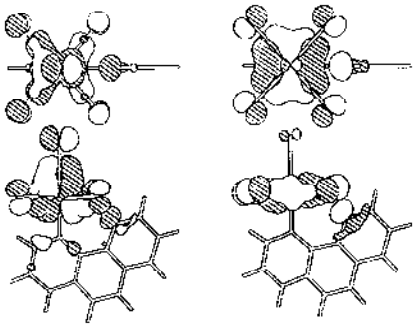

HOMO-1 HOMO-2

Fig. 5. Top and side view for HOMO-1 and HOMO-2 calculated with ZINDO/S for the capped octahedron.

Lone-pair orbitals on the "cap" nitrogen which appeared in HOMO-1 and HOMO-2 interact with MO on the central metal in an antibonding fashion as shown in Fig. 5. Thus, the "cap" nitrogen makes the intermediate unstable to accelerate Step (4). The antibonding interactions are expected to be more effective with increasing the size of the central metal. Indeed, the ordering of rates for second carbonyl extrusion was reported as Mo>W>Cr,[4,6] which clearly differs from that of dissociative reactivity of CO from $M(CO)_6$ or $M(CO)_5(L)$, Mo>Cr >W.[17,18] The acceleration at Step (3) can be explained by the idea that the mixing of two lone-pair orbitals of phen forms two new orbitals which locate energetically at a higher and lower levels compared with the originals, and the higher one coordinates to metal to release the extra energy.

According to ZINDO/S MO, visible bands of both $Cr(CO)_5$(py) (405 nm) and $Cr(CO)_5$(phen) (440 nm) were assigned to CTTL. The wavelength shift in the latter is simply due to the fact that LUMO (phen) locates at a lower level than LUMO (py) does.

This work was partly supported by a Grant-in-Aid for Scientific Research from the Ministry of Education, Science and Culture of Japan (No. 03303001 and 05640670).

REFERENCES

1 Dedicated to the memory of Professor Osamu Simamura, deceased July 9, 1993.
2 D. E. Marx and A. J. Lees, Inorg. Chem., **26**, 2254(1987).
3 R. J. Kazlauskas and M. S. Wrighton, J. Am. Chem. Soc., **104**, 5784(1982).
4 S. Oishi, Organometallics, **7**, 1237(1988).
5 K. B. Reddy, R. Hoffmann, G. Konya, R. van Eldic, and E. M. Eyring, Organometallics, **11**, 2319(1992).
6 S. Zhang, V. Zang, G. R. Dobson, and R. van Eldic, Inorg. Chem., **30**, 355(1991).
7 S. Oishi and T. Kawashima, Chem. Lett., 747(1992).
8 S. Oishi, M. Watanabe, and T. Muraishi, Chem. Lett., 713(1993).
9 F. A. Cotton and C. S. Kraihanzel, J. Am. Chem. Soc., **84**, 4432(1962).
10 J. A. Timney, Inorg. Chem., **18**, 2502(1979).
11 R. N. Perutz and J. J. Turner, Inorg. Chem., **14**, 262(1962).
12 F. Basolo and R. G. Pearson, "Mechanism of Inorganic Reactions. A Study of Metal Complexes in Solution," Wiley, New York (1958), pp145-158.
13 M. G. B. Drew, Prog. Inorg. Chem., **23**, 67(1977).
14 K. B. Wiberg, Tetrahedron, **24**, 1083(1968).
15 CAChe work system, ver., 3.0.4.1. CAChe Scientific.
16 E. W. Abel and I. S. Butler, Trans. Faraday Soc., **63**, 45(1967).
17 W. D. Covey and T. L. Brown, Inorg. Chem., **12**, 2820(1973).
18 D. Darensboug, Adv. Organomet. Chem., **21**, 113(1982).